
Joint
Quantum
Centre
WWW.JQC.ORG.UK


Newcastle
University

Atom–Light Interactions

JQC Graduate Course, Durham University
and Newcastle University

2021

Contents

Dr Tom Billam
thomas.billam@newcastle.ac.uk
Room 2.15 Herschel Annexe

0 Preliminaries

0.1 Aims of the course

An incredibly broad range of physics can be accessed with atoms and coherent laser light, and developing a completely rigorous understanding of many of the observable physical effects requires going to considerable depth[1]. The intent of this course is unashamedly practical, with an emphasis on presenting some of the powerful effective models for atoms, light, and their interaction and developing the ability to use them to do practical calculations. Rigorous and detailed derivations of the models can be found in other places.

[1] The book of Cohen-Tannoudji *et al.*, for example, devotes $\sim 10^2$ pages just to *deriving* the master equation for a two-level atom coupled to the vacuum EM field.

With the emphasis on practical calculations comes the necessity to model things numerically using a computer, and the course problems will sometimes require you to do this. Over the duration of the course, two key computational procedures will occur quite frequently, so we shall review them now:[2]

[2] A note on programming languages: in the notes and lectures I will demonstrate examples in python, using the `numpy` and `scipy` libraries. These are open-source and widely available. If you prefer to work through the problems in another language (e.g., Matlab, Mathematica, Fortran, C/C++) this is also fine, but bear in mind that your colleagues and I may be less able to help you with any coding difficulties.

0.2 Numerical solution of coupled ODEs

We will frequently find models for the behaviour of atom-light systems that can be expressed as coupled ordinary differential equations (ODEs). Typically these will appear in the form of an initial value problem (IVP) where

$$\frac{d\mathbf{u}}{dt} = \mathbf{f}(\mathbf{u}, t)\,, \tag{1}$$

and one seeks the solution $\mathbf{u}(t_0 + t)$, given a specified initial condition $\mathbf{u}(t_0) = \mathbf{u}_0$.

Let us explore the numerical solution of such a system using the example of a rigid pendulum. In this case we have the second-order ODE[3]

[3] Made dimensionless for simplicity; see virtually any mechanics text book for details!

$$\frac{d^2\theta}{dt^2} = -\sin(\theta)\,. \tag{2}$$

As an example of a general principle, this second-order equation can be reduced to two *coupled* first-order equations:

$$\frac{d\theta}{dt} = \dot{\theta}\,, \quad \frac{d\dot{\theta}}{dt} = -\sin(\theta)\,. \tag{3}$$

This matches our general definition [Eq. (1)] if we set the components of the vector $\mathbf{u}$ such that $\mathbf{u} = (\theta, \dot{\theta})$.

Let us solve this for the initial condition $\theta(t = t_0 = 0) = \pi/4$ and $\dot{\theta}(t = t_0 = 0) = 0$. The following minimal python program does this and plots the solution to a graphical window:

```
from scipy.integrate import ode
from numpy import sin, zeros, linspace, pi
import matplotlib.pyplot as plt

# --- Getting latex to work for figure labels ---
from matplotlib import rc
rc('font',**{'family':'serif','serif':['Palatino']})
rc('text', usetex=True)
# -----------------------------------------------

# Create a function that returns a vector of derivatives
def f(t, u):
  return [u[1], -sin(u[0])]

# Create an integrator object, using the Dormand-Prince
# 4-5 order Runge-Kutta method
i = ode(f).set_integrator('dopri5',
                          atol=1E-6,
                          rtol=1E-6,
                          first_step=1.0E-6)

# Create a vector of times at which we want the solution
tMax = 2.0*pi
nPoints = 100
dt = tMax / (nPoints-1)
tArr = linspace(0,tMax,nPoints,endpoint=True)

# Create an empty vector to hold the solution
uArr = zeros((nPoints,2))

# Initial condition
uArr[0,:] = [pi/4.0, 0.0]
i.set_initial_value(uArr[0,:], tArr[0])

# Integrate equation in steps to fill our array
for j in range(0,nPoints-1):
  uArr[j+1,:] = i.integrate(i.t+dt)
  if (i.successful()==False):
    break

# Plot the solution
```

```
plt.plot(tArr/(2.0*pi),uArr[:,0]/pi)
plt.xlabel(r'$t/2\pi$')
plt.ylabel(r'$\theta/\pi$')
plt.show()
```

The above program provides a skeleton to work with if you are unsure of how to start. Some comments:

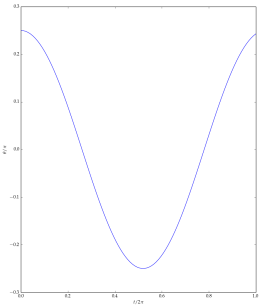

Figure 1: Example output from the ODE-solving program.

- Many numerical packages provide a wide choice of numerical integrators (and, of course, you can directly code your own). A good rule of thumb is to start with a 4th-5th order adaptive Runge-Kutta method, and only worry about other schemes if that fails!
- As you can see, using python with `numpy` and `scipy` is fairly terse. To learn about what the various functions and classes do, and what the options are, consult the extensive online documentation (e.g., here).

0.3 Matrix representations of quantum mechanics

A second recurring theme will be dealing with finite-dimensional quantum mechanical operators numerically: particularly angular momentum operators. As an example of how to do this, let us consider the perennial example of a spin-1/2 system[4]. We shall go through the mapping to matrix algebra step-by-step here.

[4] See, e.g., Levin's *"An Introduction to Quantum Theory"* for a reminder of the physics if necessary.

Representation of states

The two possible states of a spin-1/2 system, given a fixed z-axis, are spin-up, denoted $|+\frac{1}{2}\rangle$, and spin-down, denoted $|-\frac{1}{2}\rangle$. A general state of the system can thus be encoded as a two-component vector

$$|\psi\rangle = c_+|+\tfrac{1}{2}\rangle + c_-|-\tfrac{1}{2}\rangle \quad \leftrightarrow \quad \boldsymbol{\psi} = \begin{pmatrix} c_+ \\ c_- \end{pmatrix}. \tag{4}$$

Representation of operators

The spin-up and spin-down states are defined as eigenstates of the dimensionless z-spin projection operator $\hat{s}_z$, such that[5]

[5] As in the main notes, I here adopt the convention that the expected dimensionful z-component of the angular momentum of a state $|\psi\rangle$ is given by $\langle\psi|\hbar\hat{s}_z|\psi\rangle$. This avoids an awful lot of $\hbar$'s in the equations!

$$\hat{s}_z|\pm\tfrac{1}{2}\rangle = \pm\frac{1}{2}|\pm\tfrac{1}{2}\rangle\,. \tag{5}$$

The matrix representation for $\hat{s}_z$ is thus

$$\mathfrak{s}_z = \frac{1}{2}\begin{pmatrix} 1 & 0 \\ 0 & -1 \end{pmatrix}, \tag{6}$$

and the $\hat{s}_x$ and $\hat{s}_y$ operators are represented by the other two *Pauli matrices*

$$\mathfrak{s}_x = \frac{1}{2}\begin{pmatrix} 0 & 1 \\ 1 & 0 \end{pmatrix} \quad \mathfrak{s}_y = \frac{1}{2}\begin{pmatrix} 0 & -i \\ i & 0 \end{pmatrix}. \tag{7}$$

Raising and lowering operators

While these operators are simple enough to remember for spin-1/2, it is useful to consider a general algorithm to construct them for higher angular momenta. This can be achieved using the **raising** and **lowering** operators, $\hat{s}_+$ and $\hat{s}_-$, where

$$\hat{s}_\pm = \hat{s}_x \pm i\hat{s}_y\,. \tag{8}$$

To determine their matrix representation, we will consider the action of the equivalent operators in a more general spin-j space, with orthonormal eigenstates defined by $|m_j\rangle$[6] and operators $\hat{j}_z$ etc. Then,

$$\hat{j}_\pm|m_j\rangle = \sqrt{j(j+1) - m_j(m_j \pm 1)}\,|m_j \pm 1\rangle\,. \tag{9}$$

A bit of close inspection shows that the general $\mathfrak{j}_+$ matrix can thus be generated by the following algorithm (given here as a python function):

[6] In these terms, spin-1/2 corresponds to $j = \frac{1}{2}$, and the possible values of the projection quantum number are given by $m_j = \pm\frac{1}{2}$. More generally, m_j can take the $2j+1$ allowed values of $-j, -j+1, \ldots, j-1, j$.

```
# Get functions from numpy
from numpy import zeros, rint

# Raising operator
def Jplus(j):
  dim = rint(2.0*j+1).astype(int) # <-- round 2j+1 to integer
  jp = zeros((dim,dim))
  for mj in range(dim-1):
    jp[mj,mj+1]=sqrt(j*(j+1)-(j-mj)*(j-mj-1))
  return jp
```

The general j_- matrix is simply given by the transpose of this. Thus, for $j = \frac{1}{2}$ we have[7]

[7] If you aren't convinced, try the code yourself!

$$j_+ = \begin{pmatrix} 0 & 1 \\ 0 & 0 \end{pmatrix}. \tag{10}$$

Having made the general raising and lowering operators, all the other operators can be formed easily via the relations (using the general notation for spin-j here)

$$j_x = \frac{1}{2}(j_- + j_+), \quad j_y = \frac{i}{2}(j_- - j_+), \quad j_z = \frac{1}{2}(j_+ j_- - j_- j_+). \tag{11}$$

Tensor products

A large part of the structure of energy levels in atoms arises from terms in the Hamiltonian which couple different angular momenta together. The state-space necessary to describe the coupling between two such angular momenta is a *tensor product* of their individual state spaces. Let us explore this for the case of two spin-1/2 angular momenta[8]. It will help to label our spins A and B, and we shall write states of the combined system as

[8] This isn't an entirely academic example; it is physically relevant for the hyperfine structure of the Hydrogen ground state, for example.

$$|\psi\rangle = c_{++}|+\tfrac{1}{2},+\tfrac{1}{2}\rangle + c_{+-}|+\tfrac{1}{2},-\tfrac{1}{2}\rangle + c_{-+}|-\tfrac{1}{2},+\tfrac{1}{2}\rangle + c_{--}|-\tfrac{1}{2},-\tfrac{1}{2}\rangle, \tag{12}$$

or in vector form as

$$\psi = \begin{pmatrix} c_{++} \\ c_{+-} \\ c_{-+} \\ c_{--} \end{pmatrix}, \tag{13}$$

where $|m_A, m_B\rangle$ denotes a simple product[9] of system A in state m_A and system B in state m_B. In the field of angular momentum this new space, constructed from all possible products of the basis states of the subspaces, is termed the **uncoupled basis**.

To describe operators in this uncoupled basis, we just take Kronecker[10] (outer) products of their matrix representations in the relevant subspace. For example, the total spin z-projection operator $\hat{S}_z = \hat{s}_{A_z} + \hat{s}_{B_z}$ can be represented by the matrix

$$\mathcal{S}_z = \mathfrak{s}_{A_z} \otimes \mathbb{I}_B + \mathbb{I}_A \otimes \mathfrak{s}_{B_z}, \tag{14}$$

where $\mathbb{I}$ denotes the identity matrix. We can let python work this one out by extending the example above:

```
# Get functions from numpy
from numpy import zeros, rint, sqrt
from numpy import transpose, kron, dot, identity

# Raising operator
def Jplus(j):
  dim = rint(2.0*j+1).astype(int) # <-- round 2j+1 to integer
  jp = zeros((dim,dim))
  for mj in range(dim-1):
    jp[mj,mj+1]=sqrt(j*(j+1)-(j-mj)*(j-mj-1))
  return jp

# Single spin operator
ap = Jplus(0.5)
am = transpose(ap)
az = 0.5*(dot(ap,am)-dot(am,ap))

# Total spin operator
sz = kron(az,identity(2)) + kron(identity(2),az)

print sz
```

This yields

[9] Note that although these basis states are product states, we can use them to construct entangled states such as the state $(|+\frac{1}{2},-\frac{1}{2}\rangle - |-\frac{1}{2},+\frac{1}{2}\rangle)/\sqrt{2}$.

[10] The Kronecker product of two matrices $\mathcal{A}$ and $\mathcal{B}$ consists of replacing each entry of $\mathcal{A}$, which are complex numbers a_{ij}, with the complex *matrix* $a_{ij}\mathcal{B}$.

$$\mathcal{S}_z = \begin{pmatrix} 1 & 0 & 0 & 0 \\ 0 & 0 & 0 & 0 \\ 0 & 0 & 0 & 0 \\ 0 & 0 & 0 & -1 \end{pmatrix}, \tag{15}$$

as one would hope!

The coupled basis and Clebsch-Gordon coefficients

Depending on the Hamiltonian under consideration, when dealing with coupled angular momenta it can be easier to switch from the uncoupled basis of $|m_A, m_B\rangle$ states to the **coupled basis** of $|S, M_S\rangle$ states. The latter are the simultaneous eigenstates of the total angular momentum squared $\hat{S}^2$ and the z-projection of the total angular momentum $\hat{S}_z$. The mapping between the coupled and uncoupled states is expressed by the **Clebsch-Gordon** coefficients

$$\langle m_A, m_B | S, M_S \rangle \,. \tag{16}$$

A conceptually and computationally convenient way to find all the Clebsch–Gordon coefficients for a given mapping between bases is as follows:

1. Proceed as we have done above, and construct the *operators* $\hat{S}^2$ and $\hat{S}_z$ in the uncoupled basis.
2. Diagonalize the operator $\hat{\Xi} = \hat{S}^2 + \hat{S}_z$ to find normalized eigenstates. Each of these eigenstates $|\xi\rangle$ will have good eigenvalues S and M_S, and thus correspond to a coupled basis state $|S, M_S\rangle$.
3. For each eigenstate $|\xi\rangle$, find its quantum numbers in the coupled basis via $S(S+1) = \langle \xi | \hat{S}^2 | \xi \rangle$ and $M_S = \langle \xi | \hat{S}_z | \xi \rangle$.
4. The vector entries of the eigenstate corresponding to $|S, M_S\rangle$ are nothing other than the Clebsch-Gordon coefficients $\langle m_A, m_B | S, M_S \rangle$.

1 Atoms in zero field

1.1 Gross and fine structure

Atomic structure in general is an exceedingly rich field with many subtleties, especially when one considers heavy, many-electron atoms. Attempting to derive an ab-initio description of a complex atom starting from relativistic quantum electrodynamics (QED) is pretty much hopeless[11]. However, as evidenced by the widespread adoption of alkali and alkali-earth atom ensembles as the building blocks for controlled quantum systems, in these simpler atoms, at sufficiently low energies and densities, many of the complex details of atomic internals can be very accurately parametrized by coefficients in a coarser, and simpler, effective model.

[11] And since, as we shall see, the electrons are always interacting with the nucleus, one could convincingly argue that a true ab-initio description of an atom should start with an ab-initio description of the nucleus!

In this section I will give an overview of an effective model that is sufficient to understand an extremely wide range of atomic spectroscopy experiments. I will also try to highlight the physics underlying some of the terms which appear more or less "phenomenologically" in this model, and the places where assumptions have been made that might, in some situations, need to be revisited.

1.1.1 One electron: Hydrogen

Non-relativistic energy levels: the Schrödinger picture

The starting point for an effective description of Hydrogen is the non-relativistic Schrödinger equation for a point-particle electron[12]:

[12] See, e.g., Foot Ch. 2, or Woodgate Ch. 2.

$$\left[-\frac{\hbar^2}{2\mu}\nabla^2 + V(\mathbf{r}) - E\right]\psi(\mathbf{r}) = 0\,. \tag{17}$$

To model Hydrogen, one should use the Coulomb potential

$$V(\mathbf{r}) = V(r) = \frac{-e^2}{4\pi\epsilon_0 r}\,, \tag{18}$$

and one can take $\mu = m_e m_p/(m_e + m_p) \approx m_e$. Two key features of this potential are:

1. It is spherically symmetric: in spherical polar coordinates $V(\mathbf{r}) = V(r)$.

2. It is *attractive*, leading to bound states.

The first of these features leads directly to the angular momentum structure of Hydrogen and the alkalis. To see this, rewrite the derivative term in spherical polars as

$$\nabla^2 = \frac{1}{r^2}\frac{\partial}{\partial r}\left(r^2\frac{\partial}{\partial r}\right) - \frac{1}{r^2}\ell^2\,, \tag{19}$$

where

$$\ell^2 = -\left[\frac{1}{\sin\theta}\frac{\partial}{\partial\theta}\left(\sin\theta\frac{\partial}{\partial\theta}\right) + \frac{1}{\sin^2\theta}\frac{\partial^2}{\partial\phi^2}\right] \tag{20}$$

is the coordinate representation of the dimensionless[13] angular momentum operator $\hat{l}^2$. The eigenfunctions of ℓ are the spherical harmonics $Y_{l,m_l}(\theta,\phi)$: the quantum numbers l and m_l for these functions satisfy

$$\ell^2 Y_{l,m_l}(\theta,\phi) = l(l+1)Y_{l,m_l}(\theta,\phi)\,, \tag{21}$$

for integer l, and

$$\ell_z Y_{l,m_l}(\theta,\phi) = m_l Y_{l,m_l}(\theta,\phi)\,, \tag{22}$$

for integer m_l, where $\ell_z = -i\partial/\partial\phi$ is the coordinate representation of $\hat{l}_z$, the angular momentum projection on the z-axis. A more careful consideration of spherical harmonics reveals the rule that $-l \le m_l \le l$.

Returning to Eq. (17), it is clear that we can make the separation $\psi(\mathbf{r}) = R(r)Y(\theta,\phi)$. This leaves us with the defining equation of the spherical harmonics, which gives rise to the algebra of angular momentum, and the *radial equation*

$$\left[-\frac{1}{r^2}\frac{\partial}{\partial r}\left(r^2\frac{\partial}{\partial r}\right) + \frac{2m_e}{\hbar^2}\left(V(r)-E\right) + \frac{l(l+1)}{r^2}\right]R(r) = 0\,. \tag{23}$$

Working through the solution to Eq. (23) analytically is quite long but perfectly possible[14], and one obtains

[13] We will adopt the convention that the expected dimensionful z-component of the angular momentum of a state $|\psi\rangle$ is given by $\langle\psi|\hbar\hat{l}_z|\psi\rangle$, and an eigenstate obeys $\hat{l}_z|l,m_l\rangle = m_l|l,m_l\rangle$. This definition avoids an awful lot of $\hbar$'s in the following equations.

[14] See, e.g., Ch. 11 of Levin

$$R_{nl}(r) = \frac{2a_0^{-3/2}}{n^2}\sqrt{\frac{(n-l-1)!}{(n+l)!}}\left(\frac{2r}{na_0}\right)^l L_{n-l-1}^{2l+1}\left(\frac{2r}{na_0}\right)e^{-r/na_0}\,, \tag{24}$$

where $L_{n-l-1}^{2l+1}(x)$ is an associated Laguerre polynomial, and

$$a_0 = \frac{4\pi\epsilon_0\hbar^2}{m_e e^2} \tag{25}$$

is the Bohr radius. A few further important facts emerge from this calculation:

1. The principle quantum number $n > 0$ determines the energy, via

$$E_n = -\frac{1}{2n^2}\frac{e^2}{4\pi\epsilon_0 a_0} = -\frac{hc}{n^2}R_\infty\,, \tag{26}$$

   where $R_\infty = m_e e^4/8\epsilon_0^2 h^3 c$ is the **Rydberg constant**. The fact that the energy is independent of l (leading to high degeneracy) is a special feature of $1/r$ potentials.

2. The angular momentum quantum number l obeys $l<n$.

3. For given n, l, the radial part of the wavefunction has $n-l-1$ nodes.

Beyond the Schrödinger picture: the Dirac picture

While the non-relativistic Schrödinger equation is of great use in motivating the general energy level structure of Hydrogen, it is, unsurprisingly, not the full story. A more complete description is provided by the Dirac equation for an electron bound in the $1/r$ Coulomb potential. This introduces relativistic effects into the model, in particular the fact that the electron has *spin*.

Without going into much detail here[15], we will note that the leading-order terms when expanding the Dirac equation about the non-relativistic limit are of the form

[15] See, e.g., Woodgate Ch. 4 for a bit more detail than given here (but still not the full calculation).

$$H' = H_{\text{Spin-Orbit}} + H_{\text{Kinetic}} + H_{\text{Darwin}}$$
$$= \frac{1}{2}\frac{e^2}{4\pi\epsilon_0}\frac{\hbar^2}{m_e^2c^2}\frac{g_s}{2}\frac{\hat{\mathbf{l}}\cdot\hat{\mathbf{s}}}{r^3} - \frac{\hat{p}^4}{8m_e^3c^2} + \frac{4\pi\hbar^2}{8m_e^2c^2}\frac{e^2}{4\pi\epsilon_0}\delta(\mathbf{r})\,. \tag{27}$$

Here g_s is the spin g-factor for the electron, which we will generally assume to be $g_s = 2$.[16] Note that the spin-orbit term affects only states with $l > 0$, giving energy shifts

[16] Technically there is a QED correction: $g_s = 2[1 + (1/2)(\alpha/\pi) - 0.32848(\alpha/\pi)^2 + \ldots]$, where $\alpha = e^2/4\pi\epsilon_0\hbar c \approx 1/137$ is the fine structure constant.

$$\Delta E_n^{\text{spin-orbit}}(l) = \frac{\alpha^2}{nl(l+1)}E_n\,, \tag{28}$$

where $\alpha = e^2/4\pi\epsilon_0\hbar c \approx 1/137$ is the fine structure constant. The *Darwin* term only affects the $l = 0$ electron states which overlap the nucleus.

The combined effect of these terms is a shift of the Schrödinger energy levels by

$$\Delta E_{nj} = \frac{1}{2}m_e c^2\left(\frac{\alpha}{n}\right)^4\left(\frac{3}{4} - \frac{n}{j+\frac{1}{2}}\right), \tag{29}$$

where j is quantum the number for the total angular momentum $\hat{\mathbf{j}} = \hat{\mathbf{l}} + \hat{\mathbf{s}}$.

Notation for energy levels

The splitting of the degenerate Schrödinger energy levels according to j in the Dirac picture is termed **fine structure**, since it was first noticed (prior to the development of the Dirac theory!) as a narrow splitting of spectral lines. Indeed, the work of old spectroscopists lives on in the way in which atomic energy levels are described: The spectroscopic notation for single-electron atoms is given in the form $nl\,^{2s+1}l_j$, where the actual value of l is converted to a letter according to the recipe $0 = s$, $1 = p$, $3 = d$, $4 = f$, $5 = g$, $6 = h$,....

The first part of this expression, nl, is called the **configuration**, which defines the spatial "orbital" in which the electron being described resides. The second part, $^{2s+1}l_j$, is called the **term**, and defines the way that the spin and the orbital angular momentum are mutually configured. Note that the letter standing for l is capitalized. It is also important to remember that there are multiple degenerate states that fall within a spectroscopic **term**, with different m_j values.

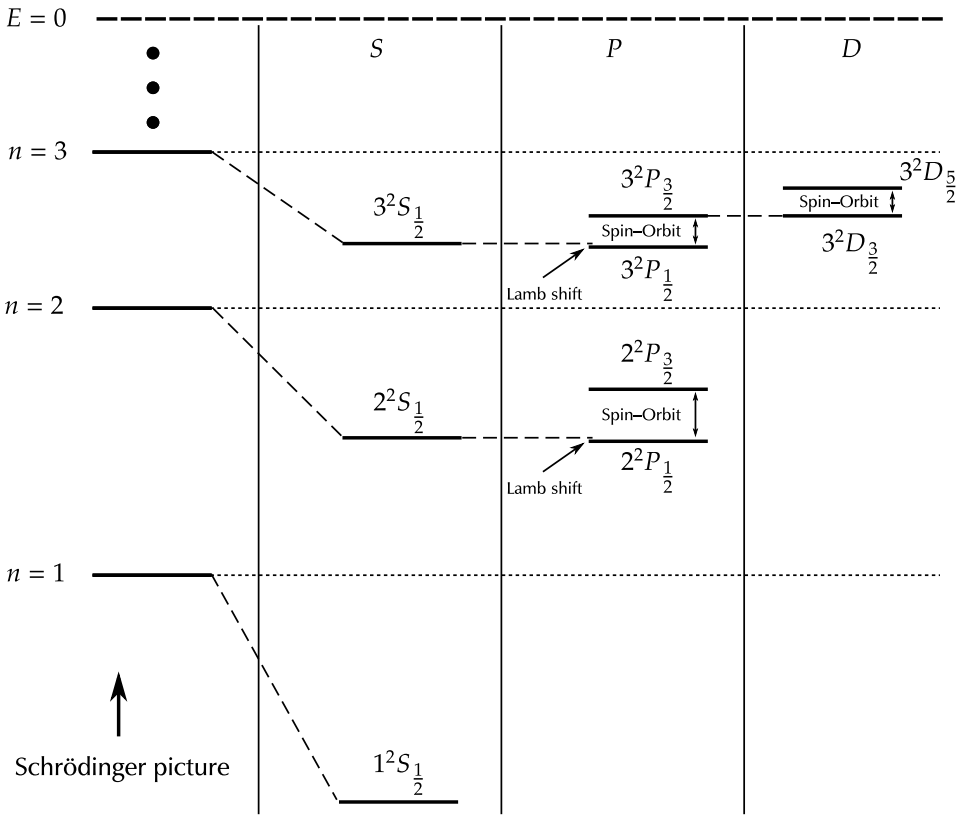

Figure 2: Schematic (not to scale) of the energy level structure of Hydrogen including relativstic terms and fine structure, and indicating the Lamb shift. Hyperfine structure (similar in energy to the Lamb shift) is not shown.

This leads to the energy level structure for Hydrogen shown in Fig. 2. Note that in single-valence-electron atoms, one often sees the configuration-term notation shortened to nl_j (with L letter capitalized), since $2s + 1$ is always 2 and there is no point repeating l.

Beyond Dirac!

As you can see in Fig. 2, and deduce easily from Eq. (29), the Dirac equation treatment predicts degenerate energies for the $2S_{\frac{1}{2}}$ and $2P_{\frac{1}{2}}$ term (or any other terms with equal n and j but differing l). However, experiments show an energy shift of $\sim 1\,\text{GHz}$ between these levels. This **Lamb shift** can described to extremely high precision by a QED treatment of the interactions between the electron and the vacuum state of the electromagnetic field.

1.1.2 Multi-electron atoms with one valence electron: The alkalis

Bottom-up treatment: central potentials

An alkali atom with atomic number Z features $Z - 1$ *core* electrons in

closed (filled) shells around the nucleus, with a single valence electron outside. This valence electron moves in a combined potential due to the nucleus and all the core electrons. If one seeks a quantitatively predictive treatment, one should also worry about the influence of the valence electron on the potential experienced by the core electrons; this can be taken into account using a self-consistent Hartee method if necessary[17].

[17] See, e.g., Woodgate for more details.

For our purposes, however, it is sufficient to consider a much simpler model[18], in which the valence electron moves in a fixed effective central (i.e., only r-dependent) potential. At large r, this potential must tend to the Coulomb potential for the *net* charge of the nucleus and core electrons, giving $V_C(r) \to -e^2/4\pi\epsilon_0 r$. Very close to the nucleus, effectively *inside* the core electrons, one should have $V_C(r) \to -Ze^2/4\pi\epsilon_0 r + C$, where C is some constant.

[18] Also described in Ch. 4 of Foot.

An approximate quantitative form for the potential in the crossover region is given by the Thomas-Fermi method[19]. Finding central potentials which give *accurate* predictions of the energy levels for a given atom is something of an art; the best models have many terms with coefficients chosen to fit the measured spectra. However, one property of central potentials in particular leads to a helpful structure of the energy levels:

[19] See e.g., Woodgate Ch. 6

Top-down treatment: quantum defects

Two key qualitative feature of any central potential describing an alkali atom are that:

- The changes from the Hydrogenic $1/r$ potential are confined to the core region at small r.
- The core potential has a large magnitude compared to the more extensive $1/r$ potential.

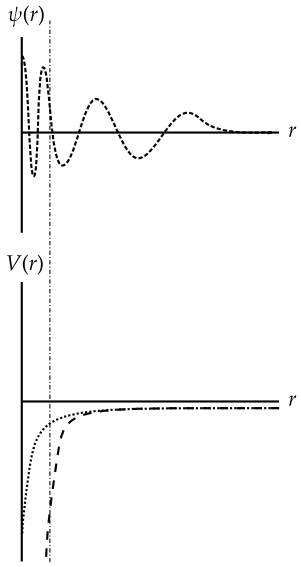

Figure 3: Effects of a strong core potential (lower, dashed) with a $1/r$ tail (lower, dotted): the wavefunction inside the core region (dot-dashed line) is quite insensitive to E, leading to the quantum defect formula.

If we consider the solutions of the radial equation as a *continuous* function of E (these will of course diverge when E isn't an eigenvalue!), this structure of the potential has the consequence that the wavefunctions are much more sensitive to the value of E in the $1/r$ tail region at large r than they are in the core region at small r(see Fig. 3). One thus generically finds that the new eigenfunctions in the central potential can be found by shifting the hydrogenic eigenvalues. In general, the new energy levels are thus given by the formula

$$E_{nl} = -\frac{hcR_\infty}{(n-\delta_l)^2}\,, \tag{30}$$

where δ_l is the **quantum defect**. One can also define the *effective quantum number*

$$n^* = n - \delta_l \,. \tag{31}$$

This is l-dependent since high-angular-momentum electrons experience the core potential less[20]. It is also weakly n-dependent for low n. Importantly, however, the δ_l are measurable quantities for a given atom, which one can look up and use!

[20] δ_l is in general insignificant for $l > 2$.

Fine structure

Of the three corrections to non-relativistic quantum mechanics predicted by the Dirac equation for hydrogen, only the spin-orbit coupling remains a significant effect in the heavier alkali atoms. Similar reasoning as to the effects of the central potential apply to the expectation value of the spin-orbit interaction as to the atomic energy levels themselves, such that the fine structure splitting between $j = l + 1/2$ and $j = l - 1/2$ levels is approximately given by the **Landé formula**

$$\Delta E_{nl} = hcR_\infty \alpha^2 \frac{Z^2}{n^{*3} l(l+1)} \,. \tag{32}$$

1.1.3 Multiple valence electrons

Here we shall mention for completeness some of the features of multiple-valence-electron atoms such as Sr, although we will not delve too much into their details in this course.

LS-coupling

Often, the structure of multiple-valence-electron atoms bears much similarity to the simpler alkalis if one considers, instead of $\hat{l}$ and $\hat{s}$, the *sums* of orbital and spin angular momentum, namely

$$\hat{\mathbf{L}} = \sum_{i=1}^{N} \hat{\mathbf{l}}_i \,, \tag{33}$$

and

$$\hat{\mathbf{S}} = \sum_{i=1}^{N} \hat{\mathbf{s}}_i \,. \tag{34}$$

This LS-coupling works well when spin-orbit interactions are small compared to the electrostatic interaction energy between the valence electrons[21]. Fine structure leads to energy levels depending on the total angular momentum $\hat{\mathbf{J}} = \hat{\mathbf{L}} + \hat{\mathbf{S}}$, with good quantum numbers J and M_J replacing M_S and M_L. Thus we may now notate the terms for a given set of individual electron configurations by $n_1 l_1 \ldots n_N l_N \, {}^{2S+1}L_J$. **Note that we will adopt the LS coupling notation for all atoms from this point forward.**

[21] See, e.g., Foot Ch.5.

jj-coupling

In heavier atoms the spin-orbit interaction can be significant compared to the electrostatic interaction energy between the valence electrons. In this case, one should first couple the individual spin and orbit angular momenta for each electron by defining

$$\hat{\mathbf{j}}_i = \hat{\mathbf{l}}_i + \hat{\mathbf{s}}_i \,, \tag{35}$$

before forming the total angular momentum $\hat{\mathbf{J}} = \sum_{i=1}^{N} \hat{\mathbf{j}}_i$. We will not consider the level structures for atoms in this regime any further, however.

1.2 Hyperfine structure

Up to this point, we have ignored any effects of the internal structure of the nucleus. However, the nuclear structure can have significant observable effects on the energy spectra of atoms. Here we will return to focusing on the case of single-valence-electron atoms for simplicity.

1.2.1 Nuclear magnetic dipole

Typically the largest contribution to atomic structure arises from any non-zero magnetic dipole moment of the nucleus. The nuclear dipole moment is related to the total nuclear spin, $\hat{\mathbf{I}}$, via

$$\hat{\boldsymbol{\mu}}_I = g_I \mu_N \hat{\mathbf{I}} = g_I \frac{m_e}{m_p} \mu_B \hat{\mathbf{I}}\,, \tag{36}$$

where g_I is the nuclear g-factor. The fact that the nuclear magneton μ_I is smaller than the Bohr magneton by the mass ratio between the electron and the proton means that the structure induced by this effect is at a much smaller energy scale than the fine structure splitting: hence **hyperfine structure**.

Unsurprisingly, an ab-initio calculation of the hyperfine structure is impractical. While we won't go through the derivation in detail here[22], a good approximation based around the smallness of hyperfine structure compared to fine structure leads to a hyperfine Hamiltonian

[22] See Foot Ch. 6 for a simple treatment, or Woodgate Ch. 9 for a bit more detail.

$$H_{\text{Dipole}} = A_{\text{HFS}} \hat{\mathbf{I}} \cdot \hat{\mathbf{J}}\,, \tag{37}$$

where the hyperfine structure constant A_{HFS} is measured experimentally for a given term and, of course, $\hat{\mathbf{J}} = \hat{\mathbf{L}} + \hat{\mathbf{S}}$. This approximation is exceedingly good for nearly all atomic spectroscopy experiments conducted at reasonable magnetic fields such that J is a good quantum number (see next section).

Much as the spin-orbit interaction makes it convenient to introduce $\hat{\mathbf{J}}$, and lifts the degeneracy between states with equal L and unequal J, the hyperfine interaction makes it convenient to introduce the total angular momentum $\hat{\mathbf{F}} = \hat{\mathbf{J}} + \hat{\mathbf{I}}$, and lifts the degeneracy between levels with equal J and unequal F.

1.2.2 Nuclear electric quadrupole

A second contribution to the atomic structure from the nucleus arises from the nuclear charge distribution, with the lowest-order term coming from any non-zero electric quadrupole moment of the nucleus. This moment is positive if the nuclear charge has a prolate distribution along the direction of the nuclear magnetic moment $\hat{\mathbf{I}}$, and negative if the charge distribution is oblate about this axis. The importance of this term varies between the alkalis, and the term vanishes altogether unless $I \geq 1$ and $J \geq 1$. Omitting the rather complex geometrical derivation, one finds that

$$H_{\text{Quadrupole}} = B_{\text{HFS}} \frac{3(\hat{\mathbf{I}}\cdot\hat{\mathbf{J}})^2 + \frac{3}{2}\hat{\mathbf{I}}\cdot\hat{\mathbf{J}} - \hat{I}^2\hat{J}^2}{2I(2I-1)J(2J-1)}\,, \tag{38}$$

where again B_{HFS} is an experimentally measured quantity. To an order of approximation that will suffice for the vast majority of atomic physics experiments, the total hyperfine Hamiltonian is thus $H_{\text{HFS}} = H_{\text{Dipole}} + H_{\text{Quadrupole}}$.

Exercises 1

Adding Angular momentum: two spin-$\frac{1}{2}$ and the coupled basis

Consider a system consisting of two spin-$\frac{1}{2}$ angular momenta labelled A and B:

1. Working in the uncoupled tensor-product basis for the combined system, where

$$\begin{pmatrix} c_{++} \\ c_{+-} \\ c_{-+} \\ c_{--} \end{pmatrix} \leftrightarrow c_{++}|+\tfrac{1}{2},+\tfrac{1}{2}\rangle + c_{+-}|+\tfrac{1}{2},-\tfrac{1}{2}\rangle + c_{-+}|-\tfrac{1}{2},+\tfrac{1}{2}\rangle + c_{--}|-\tfrac{1}{2},-\tfrac{1}{2}\rangle,$$

   find the 4×4 matrix representations of $\hat{S}^2$ and $\hat{S}_z$, where $\hat{\mathbf{S}} = \hat{\mathbf{s}}_A + \hat{\mathbf{s}}_B$.

   (*4 marks*)

2. The simultaneous eigenvalues and eigenvectors of the total angular momentum operators $\hat{S}^2$ and $\hat{S}_z$ can be used to define the **coupled basis**: this basis replaces the uncoupled basis states $|m_A, m_B\rangle$ with new ones $|S, M_S\rangle$ defined such that

$$\hat{S}^2|S,M_S\rangle = S(S+1)|S,M_S\rangle \quad \hat{S}_z|S,M_S\rangle = M_S|S,M_S\rangle\,.$$

   By diagonalizing a suitable matrix, find the coupled basis vectors in terms of the uncoupled ones.

   (*5 marks*)

3. Find the 4×4 matrices representing $\hat{s}_A^2$, $\hat{s}_{A_z}$, $\hat{s}_B^2$, and $\hat{s}_{B_z}$ in the uncoupled basis.

   (*2 marks*)

Adding angular momentum: general spins

Consider two angular momenta with $l = 1$, labeled A and B. Write a computer program to do the following:

5. Working in the uncoupled tensor-product basis for *both* systems where

$$\begin{pmatrix} c_{++} \\ c_{+0} \\ c_{+-} \\ \vdots \end{pmatrix} \leftrightarrow c_{++}|+1,+1\rangle + c_{+0}|+1,0\rangle + c_{+-}|+1,-1\rangle + \ldots$$

   calculate a 9x9 matrix representing $\hat{L}^2$ where $\hat{\mathbf{L}} = \hat{\mathbf{l}}_A + \hat{\mathbf{l}}_B$.

   (*4 marks*)

6. Find all Clebsch–Gordon coefficients $\langle m_A, m_B | L, M_L \rangle$

   (*5 marks*)

2 Atoms in static fields

2.1 Magnetic fields: the Zeeman effect

2.1.1 Origins

If an external magnetic field $\mathbf{B}$ is applied to an atom — which we shall without loss of generality take to be in the z-direction, $\mathbf{B} = B_z\hat{\mathbf{z}}$ — then it becomes favourable for the atoms' own magnetic moments to align with the applied field. The shifts in the energies of different magnetic moment configurations is expressed by the **Zeeman** Hamiltonian

$$\hat{H}_{\text{Zeeman}} = \mu_{\text{B}}\hat{L}_z B_z + g_s\mu_{\text{B}}\hat{S}_z B_z\,. \tag{39}$$

Note that here we have also ignored any interaction of the nuclear magnetic moment with the external field (i.e., there is no $\hat{I}_z B_z$ term); in very strong fields this would need to be revisted.

Provided the energy involved is small compared to the fine structure, such that J is a good quantum number and the angular momentum vectors $\mathbf{L}$ and $\mathbf{S}$ precess around $\mathbf{J}$, the Zeeman Hamiltonian can be written as

$$\hat{H}_{\text{Zeeman}} = \frac{\langle(\hat{\mathbf{L}} + g_s\hat{\mathbf{S}})\cdot\hat{\mathbf{J}}\rangle}{J(J+1)}\mu_{\mathbf{B}}B_z\hat{J}_z = g_J\mu_{\text{B}}B_z\hat{J}_z\,, \tag{40}$$

where the Landé g-factor is given in terms of the relevant quantum numbers

$$g_J = 1 + \frac{J(J+1) - L(L+1) + S(S+1)}{2J(J+1)}\,. \tag{41}$$

For very strong external fields the transform into terms of $\hat{\mathbf{J}}$ is not valid; only L and S are good quantum numbers. This is the **Paschen–Back** regime.

2.1.2 Zeeman effect on hyperfine structure

Weak field

In weak magnetic fields, the Zeeman Hamiltonian lifts the degeneracy between hyperfine levels with equal F and unequal M_F in a linear fashion, giving energy shifts

$$\Delta E_Z \approx g_F \mu_B B_z M_F \,, \tag{42}$$

where, in a similar way to g_J, g_F represents an average of a projection of $\hat{\mathbf{J}}$ onto $\hat{\mathbf{F}}$:

$$g_F = g_J \frac{\langle \hat{\mathbf{J}} \cdot \hat{\mathbf{F}} \rangle}{F(F+1)} = g_J \frac{F(F+1) + J(J+1) - I(I+1)}{2F(F+1)} \,. \tag{43}$$

Strong fields

In stronger fields (but not strong enough to rival fine structure effects!) the hyperfine Hamiltonian is dominated by the Zeeman Hamiltonian, and M_J, M_I become the appropriate quantum numbers instead of F and M_F. This leads to energy shifts given by

$$\Delta E_Z \approx g_J \mu_B B_z M_J \,. \tag{44}$$

This is often termed the **hyperfine Paschen–Back regime**.

Intermediate fields

While the above limits are helpful for understanding, most interesting experiments using hyperfine levels do not fall exactly in either regime. Therefore, for a given term (such as $2P_{3/2}$ in Hydrogen) it can help to study the problem non-perturbatively in the $|J, I, M_J, M_I\rangle$ basis. In this case, one constructs a matrix representation of the sum of hyperfine and Zeeman Hamiltonians for a given field, that is

$$\hat{H}_{\mathrm{HFSZ}} = \hat{H}_{\mathrm{HFS}} + \hat{H}_Z \,, \tag{45}$$

and diagonalizes to find the eigenvalues and eigenvectors. Such a calculation leads to a diagram of energy levels as a function of magnetic field,

typically referred to as a **Breit–Rabi diagram** (although Breit and Rabi only made the calculation for Hydrogen) as shown in Fig. 4. Performing such a calculation forms the core of exercise set 2.

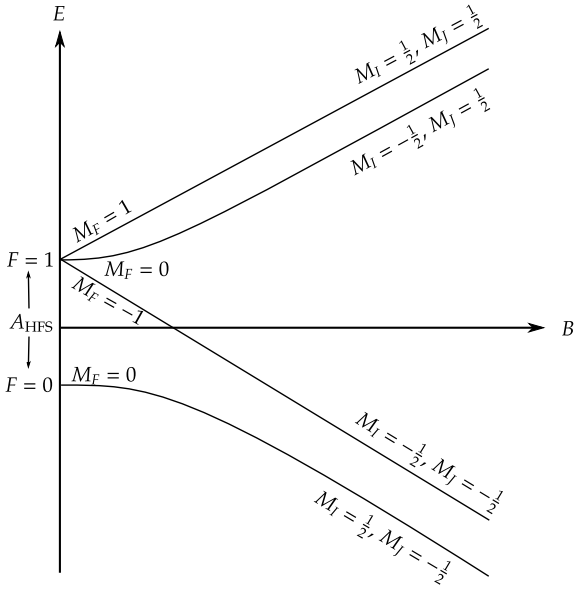

Figure 4: Schematic Breit–Rabi diagram showing the splitting of hyperfine energy levels in an applied magnetic field due to the Zeeman Hamiltonian for a $^2S_{\frac{1}{2}}$ term (after Foot, Fig. 6.10).

2.2 Electric fields: the Stark effect

An external electric field also shifts the energy eigenvalues and eigenstates of an atom. The calculation of this **Stark effect** is more involved than the above calculations for the Zeeman effect, and we will not go into any details beyond noting that the perturbing Hamiltonian is of the form

$$H_S = -\hat{\mathbf{d}} \cdot \hat{E}\,, \tag{46}$$

where $\hat{\mathbf{d}}$ is the atomic electric dipole moment operator, given in an N-valence-electron atom by

$$\hat{\mathbf{d}} = -e \sum_{i=1}^{N} \hat{r}_i\,. \tag{47}$$

Exercises 2

A generalized Breit-Rabi diagram

4. Write a code that constructs the zero-field hyperfine Hamiltonian for the $3^2P_{3/2}$ term of ^{23}Na in the $|M_J, M_I\rangle$ basis[23]. Diagonalize the resulting Hamiltonian with, and without, the electric quadrupole terms to find the resulting energy levels (in MHz).

   (*8 marks*)

5. By adding the Zeeman Hamiltonian, compute the Breit-Rabi diagram for the hyperfine Zeeman splitting of the $3^2P_{3/2}$ term, in fields of up to 100 Gauss (plot energies in MHz).

   (*8 marks*)

6. Due to space issues, a student working experimentally on the ^{23}Na D2 line finds themselves in a lab next to Prof. X's super-magnet. The ambient magnetic field strength is rising! At roughly what field strength will the $3^2P_{3/2}$ and $3^2P_{1/2}$ manifolds intersect?[24]

   (*4 marks*)

[23] You will find all necessary coefficients tabulated in Steck.

[24] Hint: you don't need to use your code to estimate this.

3 Atoms in dynamic fields

3.1 Electric dipole transitions

3.1.1 The electric dipole approximation

In order to move towards an understanding of atom-light interactions, we will first consider the interaction of an atom with a **classical**[25] time-varying electric field. The most straightforward quantitatively useful model for this interaction is the **electric dipole approximation**, in which we assume that:

[25] In essence, here we treat the electromagnetic field as a classical, time-dependent potential experienced by the atom. While this is fine for many purposes, we will see later that a much more theoretically satisfactory treatment is obtained if one also deals with the electromagnetic field on a quantum level, entering the realm of *quantum optics*.

1. We may treat the electromagnetic field as a **classical** entity described by electric and magnetic fields $\mathbf{E}(\mathbf{r}, t)$ and $\mathbf{B}(\mathbf{r}, t)$.
2. The magnetic field $\mathbf{B}(\mathbf{r}, t)$ can be neglected compared to $\mathbf{E}(\mathbf{r}, t)$; this is a good approximation for electromagnetic radiation where $\mathbf{B}(\mathbf{r}, t) \propto \mathbf{E}(\mathbf{r}, t)/c^2$.
3. The amplitude of the electromagnetic radiation varies slowly compared to its frequency ω.
4. The spatial variation of the electric field $\mathbf{E}(\mathbf{r}, t)$ is negligible over the effective diameter of the atom; this implies electromagnetic radiation with wavelengths $\lambda \gg a_0$.
5. The interaction Hamiltonian takes the form

$$\hat{H}_{\mathrm{I}}(t) = -\hat{\mathbf{d}} \cdot \mathbf{E}(\mathbf{r}_0, t)\,, \tag{48}$$

   where $\hat{\mathbf{d}}$ is the electric dipole moment operator defined in Eq. (47), and $\mathbf{r}_0$ is the location of the atom.

In this approximation we can simplify the interaction Hamiltonian further to

$$\hat{H}_{\mathrm{I}}(t) = \sum_{i=1}^{N} e\,\hat{\mathbf{r}}_i \cdot \tilde{\mathbf{e}}\,\mathscr{E}(t)\cos(\omega t)\,, \tag{49}$$

where $\tilde{\mathbf{e}}$ is a normalized polarization vector, $\mathscr{E}(t)$ is the **slowly-varying amplitude** of the electric field oscillations, which varies much slower than the angular frequency of the radiation ω. For a multiple-valence-electron atom the sum is over all the valence electrons[26].

[26] For the rest of this section we will assume a single electron and drop the summation.

3.1.2 The Rabi frequency

For simplicity, we will consider an effective two-level atom in which the levels $|e\rangle$ and $|g\rangle$ have the energies E_g and E_s. Adopting a matrix-and-vector representation based on a general state $|\psi\rangle = c_e|e\rangle + c_g|g\rangle$[27] we have

$$\mathscr{H}_{\text{atom}} = \begin{pmatrix} E_e & 0 \\ 0 & E_g \end{pmatrix} = \begin{pmatrix} E_g + \hbar\omega_0 & 0 \\ 0 & E_g \end{pmatrix}, \tag{50}$$

for the unperturbed atom, since $\langle x|\hat{H}|y\rangle = E_x\delta_{xy}$ for $x, y \in \{g, e\}$. Note that we also define here the resonance frequency $\omega_0 = (E_e - E_g)/\hbar$.

Adding in the perturbation due to the time-varying field gives

$$\mathscr{H}_{\text{atom}} + \mathscr{H}_{\text{I}} = \begin{pmatrix} E_g + \hbar\omega_0 & \hbar\Omega(t)\cos(\omega t) \\ \hbar\Omega^*(t)\cos(\omega t) & E_g \end{pmatrix}, \tag{51}$$

where we have defined the **Rabi frequency**[28]

$$\Omega(t) = \frac{\langle e|e\hat{\mathbf{r}}\cdot\tilde{\mathbf{e}}\mathscr{E}(t)|g\rangle}{\hbar}. \tag{52}$$

We shall return to the Rabi frequency and the solutions of this time-dependent Schrödinger equation in detail next time. For now, we will focus on one of its important links to atomic structure.

3.2 Selection rules

3.2.1 Selection rules for uncoupled states

Consider a stationary alkali atom at the origin of coordinates. Working in the uncoupled basis, the spatial behaviour of the valence electron is described by the quantum numbers n, l, and m_l. A key role in what follows will be played by the relative orientation of the atom with respect to the incident radiation, and we will assume that our atom is aligned with the z-axis[29]. In this case, the matrix elements defining the Rabi frequency can be written in the form

[27] See Section 0 for a recap of the details of matrix-vector representations.

[28] Note that different sources include and exclude differing factors from the Rabi frequency; there is no universally accepted definition! Leaving in the slow time-dependence due to $\mathscr{E}(t)$ will prove a notational convenience in the next lecture.

[29] In reality ensuring this requires an external magnetic field strong enough to fix this relative orientation; if such a field is not present then the results of this section must be extended by introducing averaging over relative orientations.

$$T = \langle n', l', m_l' | \hat{\mathbf{r}} \cdot \tilde{\mathbf{e}} | n, l, m_l \rangle \,. \tag{53}$$

In coordinate space this can be written as

$$T = \int_0^\infty dr \int_0^\pi d\theta \int_0^{2\pi} d\phi \, r^2 \sin(\theta) \psi^*_{n',l',m_l'}(\mathbf{r}) \, \mathbf{r} \cdot \tilde{\mathbf{e}} \, \psi_{n,l,m_l}(\mathbf{r}) \,. \tag{54}$$

For a given orientation of the polarization vector $\tilde{\mathbf{e}}$ with respect to the z-axis, the angular parts of this integral can be evaluated reasonably straightforwardly in terms of the spherical harmonics, leading to the so-called **selection rules**.

π-transitions:

For radiation with the polarization vector of the electric field parallel to the z-axis, one has $\tilde{\mathbf{e}} = \tilde{\mathbf{e}}_z$. Thus, taking the spherical polar components of $\mathbf{r}$ to be r, θ and ϕ, one has that $\mathbf{r} \cdot \tilde{\mathbf{e}} = \mathbf{r} \cdot \tilde{\mathbf{e}}_z = r\cos(\theta)$, and hence the angular part of the integral T is given by

$$I_\pi = \int_0^\pi d\theta \int_0^{2\pi} d\phi \, \sin(\theta) Y^*_{l',m_l'}(\theta,\phi) \, \cos(\theta) \, Y_{l,m_l}(\theta,\phi) \,. \tag{55}$$

From the form of the spherical harmonics

$$Y_{l,m} \propto P_l^m(\cos\theta) e^{im\phi} \,, \tag{56}$$

where P_l^m is an associated Legendre polynomial, we immediately see that the ϕ-integral imposes the condition that $I_\pi = 0$ unless $m_l' = m_l$. This defines the selection rule for π-tranisitions: $\Delta m_l = 0$.

σ-transitions:

For radiation with the polarization vector of the electric field orthogonal to the z-axis, it is convenient to write $\tilde{\mathbf{e}} = a_{\sigma^+}(\tilde{\mathbf{e}}_x + i\tilde{\mathbf{e}}_y)/\sqrt{2} + a_{\sigma^-}(\tilde{\mathbf{e}}_x - i\tilde{\mathbf{e}}_y)/\sqrt{2}$. Physically, this means splitting the polarization into left- and right-circularly polarized components (with respect to the atom[30]).

[30] Note that the correspondence between this "polarisation" of the transition and the actual polarization of the light needed to drive it depends on the propagation direction of the light!

For a pure σ^+ transition ($a_{\sigma^+} = 1, a_{\sigma^-} = 0$) we have $\mathbf{r} \cdot \tilde{\mathbf{e}} = (x + iy)/\sqrt{2} = [\sin(\theta)\cos(\phi) + i\sin(\theta)\sin(\phi)]/\sqrt{2} = \sin(\theta)e^{i\phi}/\sqrt{2}$. This gives angular integral

$$I_{\sigma^+} = \int_0^{\pi} d\theta \int_0^{2\pi} d\phi \, \sin(\theta) Y^*_{l',m'_l}(\theta,\phi) \frac{\sin(\theta)e^{i\phi}}{\sqrt{2}} Y_{l,m_l}(\theta,\phi)\,, \quad (57)$$

and again the ϕ-integral, this time over the function $e^{i(m_l+1-m'_l)\phi}$, leads to a clear selection rule that $I_{\sigma^+} = 0$ unless $\Delta m_l = 1$. For a pure σ^- transition, one obtains $I_{\sigma^-} = 0$ unless $\Delta m_l = -1$.

Selection rule for l:

In addition to the selection rules for m_l, from the angular integrals one can also derive selection rules for l. Note that[31] in terms of the spherical harmonics we can write

[31] See Foot Ch. 2 for a longer exposition.

$$\begin{aligned} z &\propto Y_{1,0}(\theta,\phi)\,, \\ x + iy &\propto Y_{1,1}(\theta,\phi)\,, \\ x - iy &\propto Y_{1,-1}(\theta,\phi)\,. \end{aligned} \quad (58)$$

Hence, we have for the angular integrals

$$I_{\Delta m_l} \propto \int_0^{\pi} d\theta \int_0^{2\pi} d\phi \, \sin(\theta) Y^*_{l',m'_l}(\theta,\phi)\, Y_{1,\Delta m_l}\, Y_{l,m_l}(\theta,\phi)\,. \quad (59)$$

Using identities for the product of spherical harmonics, one can show that $I_{\Delta m_l} = 0$ unless $l' - l = \Delta l = \pm 1$. The fact that $\Delta l = 0$ is *not* allowed is due to parity.

3.2.2 Transitions between coupled states

Because the atomic electric dipole moment arises from the position of the electron, our treatment so far has been in terms of states of well-defined l and m_l. However, as explained in previous sections, after accounting for fine and hyperfine structure, and (if present) a weak Zeeman interaction, the actual atomic energy eigenstates have well-defined values of F and M_F, and are *superpositions* of the uncoupled basis states. A transition between eigenstates therefore consists of a superposition of transitions between uncoupled basis states. Since some of these uncoupled transitions are

allowed by the selection rules while others are forbidden, the selection rules discussed above can lead to differing **relative transition strengths** among the transitions between energy eigenstates. We will investigate this further in the exercises.

Exercises 3

Selection rules:

1. An identity for the spherical harmonics $Y_{l,m_l}(\theta,\phi)$ states that

$$Y_{l,m_l}Y_{1,q} = AY_{l+1,m_l+q} + BY_{l-1,m_l+q} \tag{60}$$

for some constants A and B. Use this identity to derive the selection rule $\Delta l = \pm 1$.

(*5 marks*)

The AC Stark effect, or "light-shift":

Here we will consider the light shift in a semiclassical setting[32]. For a constant and real Rabi frequency, the two-level atom–light Hamiltonian of Eq. 51 can be written as

$$\mathcal{H}_{\text{atom-light}} = \hbar \begin{pmatrix} \omega_0 & \Omega\cos(\omega t) \\ \Omega\cos(\omega t) & 0 \end{pmatrix}. \tag{61}$$

1. Show that, after moving into a rotating frame where $|\psi\rangle = c'_e e^{-i\omega t}|e\rangle + c'_g|g\rangle$, the time-dependent Schrödinger equation can be written as

$$i\frac{d}{dt}\begin{pmatrix} c'_e \\ c'_g \end{pmatrix} = \begin{pmatrix} -\Delta & \Omega/2 \\ \Omega/2 & 0 \end{pmatrix}\begin{pmatrix} c'_e \\ c'_g \end{pmatrix}, \tag{62}$$

where $\Delta = \omega - \omega_0$ is the detuning of the optical frequency from resonance. You will need to use the **rotating wave approximation**, and discard terms of the form $e^{\pm 2i\omega t}$ from the Hamiltonian[33].

(*6 marks*)

[32] See, e.g., Foot. A much more thorough quantum-optical derivation can be found in, e.g., Cohen-Tannoudji.

[33] In somewhat hand-waving terms, one can think of this approximation as assuming that these terms "average away" over many optical cycles. More complete treatment at this semiclassical level requires Floquet analysis.

2. Diagonalize the effective Hamiltonian matrix

$$\mathscr{H}_{\text{eff}} = \begin{pmatrix} -\Delta & \Omega/2 \\ \Omega/2 & 0 \end{pmatrix}. \tag{63}$$

Plot the resulting eigenenergies as a function of Δ for; (a) $\Omega = 0.1$, (b) $\Omega = 1$, (c) $\Omega = 2$.

(*5 marks*)

3. Find an approximate expression for the eigenenergies for $|\Delta| \gg \Omega$.

(*4 marks*)

4 Semi-classical atom-light interactions

4.1 Rabi solutions

4.1.1 Time-dependent Schrödinger equation

As we have seen previously, [see Eq. (51)] the interaction of a two-level system with a classically-treated light field is governed by the time-dependent Schrödinger equation

$$i\frac{d}{dt}\begin{pmatrix} c_e \\ c_g \end{pmatrix} = \begin{pmatrix} \omega_0/2 & \Omega(t)\cos(\omega t) \\ \Omega(t)\cos(\omega t) & -\omega_0/2 \end{pmatrix}\begin{pmatrix} c_e \\ c_g \end{pmatrix}, \tag{64}$$

where we use the notation that:

$|\psi\rangle = c_e|e\rangle + c_g|g\rangle$ is the atomic state,

ω_0 is the resonance frequency of the atomic transition ($\omega_0 = \omega_e - \omega_g$),

ω is the optical frequency,

$\Omega(t)$ is the time-varying Rabi frequency[34].

[34] In this section we assume a real Rabi frequency for convenience; however, it is simple to treat a complex Rabi frequency in a similar way.

Note that we have, without any loss of generality, chosen the zero of energy to lie halfway between the atomic states. Moving to a rotating frame by writing $|\psi\rangle = c'_e e^{-i\omega t}|e\rangle + c'_g|g\rangle$, and making the rotating-wave approximation (See Exercises 3), we obtain the transformed equations

$$i\frac{d}{dt}\begin{pmatrix} c'_e \\ c'_g \end{pmatrix} = \frac{1}{2}\begin{pmatrix} -\Delta & \Omega(t) \\ \Omega(t) & \Delta \end{pmatrix}\begin{pmatrix} c'_e \\ c'_g \end{pmatrix}, \tag{65}$$

where we have defined the **detuning** $\Delta = \omega - \omega_0$.

4.1.2 Solution for a square pulse

So far, we have left the time-dependence of the Rabi frequency unspecified. A particularly experimentally-relevant case to consider is that of a square pulse of finite Rabi frequency Ω and duration τ;

$$\Omega(t) = \begin{cases} \Omega & 0 \leq t < \tau \\ 0 & \text{otherwise.} \end{cases} \tag{66}$$

In this case, one can analytically solve Eq. (65) to obtain

$$\begin{pmatrix} c'_e(\tau) \\ c'_g(\tau) \end{pmatrix} = \begin{pmatrix} \cos(\varphi) - i\frac{\Delta}{\Omega'}\sin(\varphi) & \frac{\Omega}{\Omega'}\sin(\varphi) \\ \frac{\Omega}{\Omega'}\sin(\varphi) & \cos(\varphi) + i\frac{\Delta}{\Omega'}\sin(\varphi) \end{pmatrix} \begin{pmatrix} c'_e(0) \\ c'_g(0) \end{pmatrix}, \tag{67}$$

where we have defined the **effective Rabi frequency** $\Omega' = \sqrt{\Omega^2 + \Delta^2}$, and the **pulse phase** $\varphi = \Omega'\tau/2$.

For an atom initially in the ground state $|g\rangle$ (i.e., $c'_e(0) = 0$ and $c'_g(0) = 1$) the probabilities of finding the atom in either level as a function of pulse duration simplify to

$$|c_e(\tau)|^2 = \frac{\Omega^2}{\Omega'^2}\sin^2(\varphi)\,, \quad |c_g(\tau)|^2 = \cos^2(\varphi) + \frac{\Delta^2}{\Omega'^2}\sin^2(\varphi)\,. \tag{68}$$

4.2 Density matrices

4.2.1 Density matrix formalism

Before proceeding further with our treatment of atom-light interactions, which will require us to take into account effects outside the semiclassical description, we will need to revise the use of density matrices to describe quantum systems.

An isolated quantum system described by a state vector $|\psi\rangle$ can equivalently be described by a **density matrix**[35] given by

$$\hat{\rho} = |\psi\rangle\langle\psi|\,. \tag{69}$$

Working in a basis of states $|0\rangle, |1\rangle, \ldots, |i\rangle, \ldots$ one can write the density operator explicitly as a matrix

[35] One might think it logical to call this a density *operator* in this abstract case, and only a density *matrix* when working in a specific basis. However, this hasn't traditionally been thought necessary, and even in the abstract case density *matrix* is the more popular terminology in the literature.

$$\hat{\rho} = \sum_i \sum_j |i\rangle\langle i|\hat{\rho}|j\rangle\langle j| \equiv \sum_i \sum_j |i\rangle \rho_{ij} \langle j| \,, \tag{70}$$

with elements ρ_{ij}. The density matrix allows one to calculate expectation values of operators via the basis-independent relation

$$\begin{aligned} \langle\psi|\hat{A}|\psi\rangle &= \sum_i \langle\psi|\hat{A}|i\rangle\langle i|\psi\rangle = \sum_i \langle i|\psi\rangle\langle\psi|\hat{A}|i\rangle \\ &= \sum_i \langle i|\hat{\rho}\hat{A}|i\rangle = \mathrm{Tr}[\hat{\rho}\hat{A}] \,, \end{aligned} \tag{71}$$

where Tr indicates a matrix trace (sum of diagonal entries).

Clearly for a state of the two-level system of the form $|\psi\rangle = c_e|e\rangle + c_g|g\rangle$ we would have

$$\rho = \begin{pmatrix} |c_e|^2 & c_e c_g^* \\ c_e^* c_g & |c_g|^2 \end{pmatrix} . \tag{72}$$

The diagonal terms are called populations (for obvious reasons), while the off-diagonal terms are called **coherences**. Note that the density matrix is Hermitian, and that to be physical its trace (the sum of populations) must be unity.

Inspecting this, it may not seem that we have gained much by changing description: we now have four quantities in the density matrix, but only two are independent. However, we have in fact gained the ability to write density matrices that cannot be written in terms of a wavefunction at all! For example, the density matrix

$$\rho = \begin{pmatrix} 1/2 & 0 \\ 0 & 1/2 \end{pmatrix} \tag{73}$$

does not correspond to any possible choice of c_e, c_g coefficients, but is still a perfectly valid density matrix since it is a Hermitian operator with a trace of unity. Such a density matrix corresponds to a so-called **mixed state** of the system. This represents a statistical, as well as a quantum, superposition of eigenstates[36]. Note that when mixed states are included, there are *three* degrees of freedom in the density matrix.

Because we have gained the ability to describe these mixed states, in the density matrix formalism states of the system that *can* be represented by wavefunctions are referred to as **pure states**. Mixed and pure states can

[36] At present, the utility of describing these statistical superposition states may be unclear. However, in Exercise 4 you will see how such states arise if we try observe only a subset of the degrees of freedom (e.g., a single spin) of a compound system where the degrees of freedom are entangled.

readily be distinguished by computing $\mathrm{Tr}[\hat{\rho}^2]$: for mixed states $\mathrm{Tr}[\hat{\rho}^2] < 1$, whereas for pure states $\mathrm{Tr}[\hat{\rho}^2] = 1$.

For states undergoing coherent dynamics, the density-matrix equivalent of the Schrödinger equation is the **Liouville equation**

$$i\hbar \frac{d\hat{\rho}}{dt} = \left[\hat{H}, \hat{\rho}\right] . \tag{74}$$

However, as we will see in Section 5, the density matrix formalism allows us to include incoherent, dissipative dynamics via a more general *master equation*.

4.2.2 Pseudo-spin-1/2 and the Bloch sphere

Obviously a two-level atom and a spin-1/2 system have an identical representation in terms of two-component vectors and two-by-two matrices. When dealing with the dynamics of a two-level system, it is often useful to make this **pseudospin** analogy more explicit. This can be achieved by writing all the operators in terms of the Pauli matrices $\sigma_{\{x,y,z\}}$; for example, the effective Hamiltonian for the time-dependent Schrödinger equation in the rotating frame of Eq. 65 can be written as[37]

$$H' = -\frac{1}{2}\Delta\sigma_z + \frac{1}{2}\Omega(t)\sigma_x . \tag{75}$$

[37] Note that the Pauli matrices we use here do **not** include the factor of 1/2 we included in the spin-1/2 operators $\hat{s}_{\{x,y,z\}}$.

The next logical step is to also write the density matrix itself in terms of the Pauli matrices, by defining

$$\rho(t) = \frac{1}{2}\left(\mathbf{1} + \mathbf{s}(t)\cdot\boldsymbol{\sigma}\right) . \tag{76}$$

This definition captures the three degrees of freedom present in the general density matrix in the **pseudospin vector** $\mathbf{s}(t)$.

One can easily deduce some constraints on the pseudospin vector; for pure states, $|\mathbf{s}(t)| = 1/2$, while for mixed states $|\mathbf{s}(t)| < 1/2$. Consequently, the pseudospin vector representing a general density matrix for the two-level system inhabits a unit sphere in a three-dimensional space; this is termed the **Bloch sphere**. The pure states inhabit the surface of the sphere, while the interior is made up of mixed states.

5 Spontaneous decay and the optical Bloch equations

5.1 Including spontaneous decay

5.1.1 Master equation in Linblad form

As hinted when we previously introduced the density matrix formalism, it can be used to treat the atom as a system coupled to the quantized electromagnetic field. Note that such a treatment is not really necessary for the coupling to a strong monochromatic driving field that we have considered so far; the semi-classical approach we have adopted is very accurate for this type of coupling, where one particular mode of the electromagnetic field is highly occupied.

However, what we have left out of our previous treatment is the interaction of the atom with all the other modes of the electromagnetic field. In the optical frequency range these other modes have negligible thermal occupation[38], although they do still exhibit intrinsically quantum fluctuations, commonly called vacuum noise. The coupling of the atom to all these vacuum-occupied modes of the electromagnetic field is the origin of spontaneous emission. Consequently, to correctly account for the dissipative effects of spontaneous emission we have to use a full quantum-optical treatment of all these couplings.

[38] Note that this simplification isn't available for microwaves, for example (think of the CMB).

Unfortunately, the full quantum optical treatment is beyond the scope of this eight-week course[39]. Therefore we shall bypass the long derivations and jump straight to the key result: With the other modes of the field included, the master equation for the two-level atomic density matrix takes the **Lindblad form**

[39] If time permits, I will present a brief overview of the key ideas in the lecture. Classic references on the subject are Cohen–Tannoudji, Loudon, and Scully and Zubairy.

$$\frac{d}{dt}\hat{\rho} = -\frac{i}{\hbar}\left[\hat{H},\hat{\rho}\right] + \Gamma\left(\hat{s}^{-}\hat{\rho}\hat{s}^{+} - \frac{1}{2}\hat{\rho}\hat{s}^{+}\hat{s}^{-} - \frac{1}{2}\hat{s}^{+}\hat{s}^{-}\hat{\rho}\right), \tag{77}$$

where we have introduced the **linewidth** Γ, a decay constant for the excited state, and $\hat{s}^{\pm} = \hat{s}_x \pm i\hat{s}_y$ are the spin-1/2 raising and lowering operators we encountered previously.

5.1.2 Non-driven case

While Eq. (77) might look complex, it simplifies considerably if written for the separate components of the density matrix. For a non-driven two-level

atom with natural frequency ω_0 we have

$$\hat{H} = \frac{\hbar\omega_0}{2}\hat{\sigma}_z\,, \tag{78}$$

and hence obtain

$$\frac{d}{dt}\begin{pmatrix} \rho_{ee} & \rho_{eg} \\ \rho_{ge} & \rho_{gg} \end{pmatrix} = \begin{pmatrix} -\Gamma\rho_{ee} & \left(-i\omega_0 - \frac{\Gamma}{2}\right)\rho_{eg} \\ \left(i\omega_0 - \frac{\Gamma}{2}\right)\rho_{ge} & \Gamma\rho_{ee} \end{pmatrix}. \tag{79}$$

Equation (79) makes clear the interpretation of Γ as a decay constant for the excited state. Note that the off-diagonal coherences decay at *half* the rate of the excited state population. Clearly, the only steady-state solution of Eq. (79) is the rather trivial $\rho_{gg} = 1$, and the transient solutions are not particularly exciting either.

5.1.3 Driven atom: the optical Bloch equations

Interesting steady-state and transient solutions to Eq. (77) occur when we add coherent driving into the dissipative master equation. This can be achieved using exactly the semi-classical approach we employed previously to investigate coherent driving on its own: Having transformed to an appropriate rotating frame and made the rotating wave approximation we obtain the Hamiltonian [Eq. (75)]

$$\hat{H} = -\frac{\Delta}{2}\hat{\sigma}_z + \frac{\Omega}{2}\hat{\sigma}_x\,, \tag{80}$$

and from this we find (writing components separately for clarity) the **optical Bloch equations**

$$\begin{aligned}
\frac{d}{dt}\rho_{ee} &= -\Gamma\rho_{ee} + \frac{i\Omega}{2}(\rho_{eg} - \rho_{ge})\,,\\
\frac{d}{dt}\rho_{gg} &= \Gamma\rho_{ee} - \frac{i\Omega}{2}(\rho_{eg} - \rho_{ge})\,,\\
\frac{d}{dt}\rho_{eg} &= \left(i\Delta - \frac{\Gamma}{2}\right)\rho_{eg} + \frac{i\Omega}{2}(\rho_{ee} - \rho_{gg})\,,\\
\frac{d}{dt}\rho_{ge} &= \left(-i\Delta - \frac{\Gamma}{2}\right)\rho_{ge} - \frac{i\Omega}{2}(\rho_{ee} - \rho_{gg})\,.
\end{aligned} \tag{81}$$

5.2 The optical Bloch equations

5.2.1 Pseudospin form

The coupled equations for the components of the full density matrix in Eq. (81) are often simplified by working in terms of the pseudospin vector **s** defined in Eq. (76). The components of the vector are defined by

$$s_{\{x,y,z\}} = \frac{1}{2}\mathrm{Tr}\left[\hat{\rho}\hat{\sigma}_{\{x,y,z\}}\right], \tag{82}$$

that is, the average values of the pseudospin operators. This simplifies the optical Bloch equations to three real equations:

$$\begin{aligned}
\frac{ds_x}{dt} &= \Delta s_y - \frac{\Gamma}{2}s_x, \\
\frac{ds_y}{dt} &= -\Delta s_x - \frac{\Gamma}{2}s_y - \Omega s_z, \\
\frac{ds_z}{dt} &= -\Gamma s_z + \Omega s_y - \frac{\Gamma}{2}.
\end{aligned} \tag{83}$$

These equations directly give the motion of the pseudospin vector within the Bloch sphere.

5.2.2 Steady-state solutions

Working in pseudospin form, one obtains the steady-state solutions

$$s_x = \frac{\Delta}{\Omega}\frac{S}{1+S}, \quad s_y = \frac{\Gamma}{2\Omega}\frac{S}{1+S}, \quad s_z = -\frac{1}{2(1+S)}, \tag{84}$$

where S is the **saturation** defined by

$$S = \frac{2\Omega^2}{\Gamma^2 + (2\Delta)^2}. \tag{85}$$

It is common to define S in terms of the **resonance saturation** $S_0 = 2(\Omega/\Gamma)^2$ such that

$$S = \frac{S_0}{1 + (2\Delta/\Gamma)^2}\,, \tag{86}$$

and $S = S_0$ when $\Delta = 0$. In laboratory settings the resonance saturation is usually found from the incident laser intensity I via $S_0 = I/I_{\text{sat}}$, where the I_{sat} is the **saturation intensity**

$$I_{\text{sat}} = \frac{2\pi^2\hbar\Gamma c}{3\lambda^3}\,. \tag{87}$$

From the above it is clear that the excited state population in the steady state is given by

$$\rho_{ee} = s_z + \frac{1}{2} = \frac{1}{2}\frac{S}{1+S}\,. \tag{88}$$

Physically, this means that very strong driving ($S \gg 1$) will place on average half of the atoms in the excited state.

Exercises 4

Density matrices

1. The sum of the populations in a density matrix is set to 1 initially. Show that the Liouville equation conserves this normalization for all subsequent times.

   (*2 marks*)

2. A two-level system is prepared in the state

   $$\rho = \begin{pmatrix} 3/4 & 1/4 \\ 1/4 & 1/4 \end{pmatrix}.$$

   Is this a pure state? What are the expectation values of the pseudospin operators, $\langle\hat{\sigma}_{\{x,y,z\}}\rangle$, for this state?

   (*2 marks*)

3. Two spin-1/2 systems A and B are prepared in the entangled state

   $$|\psi\rangle = \frac{1}{\sqrt{2}}\left(|+\rangle_A|+\rangle_B + |-\rangle_A|-\rangle_B\right)\,. \tag{89}$$

(a) What is the (4x4) density matrix, ρ, for this state?

(*2 marks*)

(b) By taking the **partial trace** of the matrix ρ over the degrees of freedom associated with spin B, find the (2x2) **reduced density matrix**, ρ_A, describing the effective state of spin A.

(*4 marks*)

(c) Does ρ_A represent a pure or a mixed state?

(*2 marks*)

The optical Bloch equations

5. Derive the pseudospin form of the optical Bloch equations [Eq. (83)] from the density-matrix form [Eq. (81)].

(*2 marks*)

6. Show that the pseudospin components given in Eq. (84) are a steady-state solution of the optical Bloch equations.

(*3 marks*)

7. Plot graphs of the steady-state pseudospin components $s_{\{x,y,z\}}$ as a function of Δ/Γ for resonance saturations S_0 equal to; (a) 0.01, (b) 0.1, and (c) 1.

(*3 marks*)

6 Atomic ensembles and light

In this section we will pause our consideration of the interaction of a single two-level atom with light, and briefly consider the **macroscopic properties of a medium composed of many atoms**.

6.1 Resonance fluorescence

As seen in the steady-state solutions of the optical Bloch equations that you confirmed in Exercises 4, the steady-state population of the excited state is [Eq. (88)]

$$\rho_{ee} = s_z + \frac{1}{2} = \frac{S}{2(1+S)} \,. \tag{90}$$

The linewidth Γ is, physically, a decay constant for the excited state population. Consequently if we drive an ensemble of N two-level[40] atoms close to resonance, reaching the steady-state regime, we can collect the spontaneously-emitted fluorescence photons at a rate

$$R = \epsilon N \Gamma \rho_{ee} = \epsilon N \frac{\Gamma}{2} \frac{S_0}{S_0 + 1 + (2\Delta/\Gamma)^2} \,, \tag{91}$$

where ϵ parametrizes the efficiency of detection.

Note that we may rewrite Eq. (91) as

$$R = \epsilon N \frac{\Gamma}{2} \frac{S_0}{S_0 + 1} \frac{(\gamma/2)^2}{(\gamma/2)^2 + \Delta^2} \,; \tag{92}$$

this makes clear its form as a **power-broadened Lorentzian** function of the detuning, with width[41] $\gamma = \Gamma\sqrt{S_0 + 1}$. Knowledge of this form for the fluoresence signal allows us to, for example, count the number of atoms in an ensemble experimentally.

[40] If one considers atoms with more than two levels, then the situation is more complicated if decay from the excited state to more than one lower energy level is not forbidden by selection rules.

[41] Full width at half-maximum.

6.2 Refractive index

6.2.1 Atomic dipole moment

Again starting from the steady-state solution of Eq. (88), a simple calculation shows that the expectation value of the atomic dipole moment in the direction of polarization of the driving field, $\langle \hat{\mathbf{d}} \cdot \tilde{\mathbf{e}} \rangle$ is given by[42]

$$\begin{aligned} \langle \hat{\mathbf{d}} \cdot \tilde{\mathbf{e}} \rangle &= 2\mathscr{E}\langle g|\hat{\mathbf{d}} \cdot \tilde{\mathbf{e}}|e\rangle \left[s_x \cos(\omega t) + s_y \cos(\omega t + \pi/2) \right], \\ &= 2d_{ge} \left[s_x \cos(\omega t) + s_y \cos(\omega t + \pi/2) \right] \end{aligned} \tag{93}$$

where $\mathscr{E}$ is the incident electric field amplitude encountered previously. Physically, the s_x-component of the pseudospin vector represents the induced dipole moment in phase with the driving optical field, while the s_y-component represents the induced dipole moment in *quadrature* with the driving.

[42] Note that here I am presenting a very simplified, rather than full and convincing treatment of the incident light polarization, since the latter would be quite involved.

6.2.2 Electromagnetic waves in a medium

For electrodynamics in a polarizable medium, Maxwell's equations are modified by the presence of the medium. The electric field appearing in Gauss and Ampere's laws is replaced by the electric displacement vector

$$\mathbf{D} = \varepsilon_0 \mathbf{E} + \mathbf{P} = \varepsilon_0 \mathbf{E} + \varepsilon_0 \chi \mathbf{E} = \varepsilon_r \varepsilon_0 \mathbf{E}, \tag{94}$$

where we have also defined the **polarization vector**, $\mathbf{P}$, describing the electric field induced in the medium, the **susceptibility**, χ, describing how the induced polarization varies with the driving field[43], and the **relative permittivity**, $\varepsilon_r = 1 + \chi$. Plane electromagnetic waves propagate in such a medium at the modified speed

$$\mathrm{v} = \frac{c}{\sqrt{\varepsilon_r \mu_r}} = \frac{c}{\sqrt{\varepsilon_r}} = \frac{c}{n}, \tag{95}$$

where we have assumed the relative permeability $\mu_r = 1$ at optical frequencies, and defined the **refractive index** n.

[43] Here I will consider only linear susceptibility (χ = constant), but the formalism is easily adapted to *nonlinear* susceptibilities of the form $\chi = \chi(|\mathbf{E}|)$, and less easily to anisotropic *tensor* susceptibilities. We will also ignore possible ferroelectric properties of the medium and, in keeping with the electric dipole approximation, assume its magnetic properties do not affect electromagnetic wave propagation.

Since it will be convenient to treat absorptive and dispersive properties of a medium simultaneously, we shall allow the refractive index to be complex, writing $n = n_R + in_I$. Plane electromagnetic waves in the medium then take the form $\mathbf{E}(x,t) = \mathbf{E}_0 \exp[i(n_R k_0 x - \omega t)] \exp[-k_0 n_I x]$, where k_0 is the free-space wavelength. Working in the limit of a medium with a refractive index close to one we may, in keeping with this approach, expand $n = \sqrt{1+\chi} \approx 1 + \chi/2$ and thus use the relations

$$n_R = 1 + \frac{\chi_R}{2}; \quad n_I = \frac{\chi_I}{2}. \tag{96}$$

In this approximation, the imaginary part of the susceptibility defines the absorption coefficient, while the real part determines the dispersive properties.

After careful manipulations, one can show that writing the polarization of an ensemble of atomic density n as $\mathbf{P} = n\langle \hat{\mathbf{d}} \cdot \tilde{\mathbf{e}} \rangle \tilde{\mathbf{e}}$, and using Eq. (93) and Eq. (84), leads to

$$\chi_R = -\frac{n\hbar\Omega^2}{\epsilon_0} \frac{\Delta}{\Delta^2 + (\Gamma/2)^2 + \Omega^2/2}, \tag{97}$$

$$\chi_I = \frac{n\hbar\Omega^2}{\epsilon_0} \frac{\Gamma/2}{\Delta^2 + (\Gamma/2)^2 + \Omega^2/2}. \tag{98}$$

Note that the absorptive and dispersive properties of a medium are fundamentally connected by the **Kramers-Kronig relations**

$$\chi_R(\omega) = \frac{2}{\pi} \int_0^\infty \frac{\omega' \chi_I(\omega')}{\omega'^2 - \omega^2} d\omega', \tag{99}$$

$$\chi_I(\omega) = -\frac{2\omega}{\pi} \int_0^\infty \frac{\chi_R(\omega')}{\omega'^2 - \omega^2} d\omega'. \tag{100}$$

However, further details regarding this are beyond the scope of this course[44].

[44] See Jackson's *Classical electrodynamics* or similar for more details.

6.3 Saturated absorption and the Beer-Lambert law

We now consider the propagation of a laser beam through a medium of uniform atomic density n. When passing through a thin slab of thickness

Δz, the beam will be subject to a relative loss of intensity proportional to the probability of absorption,

$$\frac{\Delta I}{I} = -n\sigma(\omega)\Delta z\,, \tag{101}$$

where $\sigma(\omega)$ is the (frequency-dependent) **absorption cross-section**. The intensity of the beam varies according to the Beer-Lambert law

$$\frac{dI}{dz} = -n\sigma(\omega)I\,. \tag{102}$$

To find $\sigma(\omega)$, we can use a simple energy-conservation argument[45]: the rate of energy absorption per unit area in a thin layer should be equal and opposite to the intensity drop in that layer. This leads us to state that [from Eq. (91) with $\epsilon = 1$]

$$\Delta I = \hbar\omega n\Gamma\rho_{ee}\Delta z \tag{103}$$

and hence

$$\frac{dI}{dz} = -\hbar\omega n\frac{\Gamma}{2}\frac{S_0}{S_0+1}\frac{(\gamma/2)^2}{\Delta^2+(\gamma/2)^2}\,. \tag{104}$$

In the low-intensity limit, $S_0 = I/I_{\rm sat} \ll 1$, and $\gamma \approx \Gamma$, and we recover the Beer-Lambert law

$$\frac{dI}{dz} = -\hbar\omega n\frac{\Gamma}{2}\frac{(\Gamma/2)^2}{\Delta^2+(\Gamma/2)^2}\frac{I}{I_{\rm sat}}\,, \tag{105}$$

with absorption cross-section

$$\sigma(\omega) = \hbar\omega\frac{\Gamma}{2I_{\rm sat}}\frac{(\Gamma/2)^2}{\Delta^2+(\Gamma/2)^2}\,. \tag{106}$$

Note that in the high-intensity limit, $S_0 \gg 1$, one obtains

[45] Note that this argument is only valid for two-level atoms in the absence of any inelastic collisional processes, which could represent another energy dissipation mechanism.

$$\frac{dI}{dz} = -\hbar\omega n\frac{\Gamma}{2}\,, \tag{107}$$

and the intensity decrease becomes *linear* in z, rather than exponential. In this regime the medium has absorbed all the photons it can, and becomes effectively transparent to any more.

Exercises 5

Optical Bloch equations: time-dependent solutions and dipole moment

1. Solve (analytically or numerically) the optical Bloch equations for a two-level system in the case of zero-detuning ($\Delta = 0$) and no initial excitation or coherence [$\rho_{ee}(0) = \rho_{eg}(0) = 0$]. Plot the excited state population as a function of time for six values of the parameter $\Gamma/\Omega = \{0, 1/4, 1/2, 1, 2, 4\}$. Show at least two Rabi cycles on each graph.

   (*5 marks*)

2. By rearranging Eq. (93) in terms of s_x/s_y, plot a graph of the phase of the atomic dipole moment relative to the driving field, as a function of the scaled detuning Δ/Γ.

   (*2 marks*)

Doppler broadening: In the notes we have considered a medium composed of *stationary* atoms. In this problem you will study the effects of atomic motion, which leads to *doppler broadening* of the absorption spectrum.

4. The intensity of light propagating through a medium in the Beer-Lambert regime has the spatial form $I = I_0 e^{-\alpha z}$, where α is the **absorption coefficient**. Express α in the form $\alpha = \alpha_0 f(\Delta, \Gamma)$, where α_0 is the detuning at $\Delta = 0$, and $f(\Delta, \Gamma)$ is a Lorentzian function with a maximum value of 1.

   (*1 marks*)

5. For an ensemble of atoms of mass m at temperature T, state (do not prove) the velocity probability distribution of the atoms on particular direction z, $P(\mathrm{v}_z)$. Quote a reference in which you found this result.

   (*2 marks*)

6. Using the fact that an atom travelling with velocity component v_z in the direction of propagation of the driving laser field experiences a Doppler-shifted effective detuning of $\Delta - kv_z$, derive an expression for the Doppler-broadened absorption coefficient α in terms of a convolution integral.

(*4 marks*)

7. Show that the full width at half-maximum of the resulting Doppler-broadened line is proportional to $\sqrt{T/m}$.

(*2 marks*)

8. Assume the 5s-5p transition in Rb at around 780nm has a width of $2\pi \times 6$ MHz. Plot: (a) the original lineshape [i.e., $f(\Delta, \Gamma)$]; (b) Doppler-broadened lineshapes for temperatures (i) 50 μK, (ii) 50 mK, (iii) 300 K.

(*4 marks*)

7 Three-level systems

In this section, we will extend our treatment of atom-light interactions to situations with more than one atomic energy level, and more than one (independent) coherent driving field. As in our treatment of the two-level system, it will be convenient first to address coherent effects using the Schrödinger equation, and subsequently to consider the effects of spontaneous emission using the optical Bloch equations.

7.1 Schrödinger picture

7.1.1 Level schemes

Unlike its two-level counterpart, the three-level system presents choices in the arrangement of the energy levels and driving fields. The three main classes of level scheme are shown in Fig. 5: the Λ, V, and *ladder* (or *cascade*) schemes. Of these, the Λ scheme exhibits the greatest range of interesting physics without too much mathematical complexity; we will focus on the nondegenerate case in what follows.

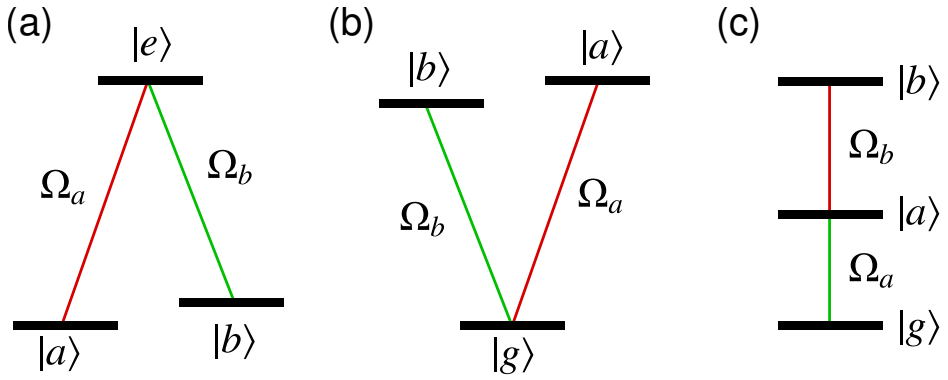

Figure 5: Common level schemes for a three-level system with two driving fields: (a) Λ, (b) V, and (c) *ladder*. Note that levels $|a\rangle$ and $|b\rangle$ in the Λ and V schemes are potentially degenerate.

7.1.2 Hamiltonian

In analogy with our previous treatment of the two-level system, we can quite straightforwardly construct the Hamiltonian for the Λ system as

$$\hat{H}_\Lambda = \hbar\omega_e^{(0)}|e\rangle\langle e| + \hbar\omega_a^{(0)}|a\rangle\langle a| + \hbar\omega_b^{(0)}|b\rangle\langle b| + \hbar\Omega_a\cos(\omega_a t)(|a\rangle\langle e| + |e\rangle\langle a|) + \hbar\Omega_b\cos(\omega_b t)(|b\rangle\langle e| + |e\rangle\langle b|)\,, \tag{108}$$

where we have defined the three energy levels by $\omega^{(0)}_{\{a,b,g\}}$, and the laser frequencies by $\omega_{\{a,b\}}$, with Rabi frequencies[46] $\Omega_{\{a,b\}}$. As in the two-level case, an appropriate choice of time-dependent expansion coefficients yields a time-dependent Schrödinger equation with time-independent Hamiltonian of the form

$$i\frac{d}{dt}\begin{pmatrix} c_a \\ c_e \\ c_b \end{pmatrix} = \frac{1}{2}\begin{pmatrix} 0 & \Omega_a & 0 \\ \Omega_a & -2\Delta & \Omega_b \\ 0 & \Omega_b & -2\delta \end{pmatrix}\begin{pmatrix} c_a \\ c_e \\ c_b \end{pmatrix}. \tag{109}$$

Note that here we have defined one detuning, $\Delta = \omega_a - (\omega_e^{(0)} - \omega_a^{(0)})$, similarly to the two-level case. However, we have defined the second detuning δ to *include* the first: $\delta = \Delta - \omega_b + (\omega_e^{(0)} - \omega_b^{(0)})$. This makes δ the net detuning of the two-photon transition from $|a\rangle$ to $|b\rangle$, giving a simpler matrix[47].

[46] Note that, as previously, we assume a real Rabi frequency to simplify later expressions. The generalization to complex Rabi frequency is straightforward.

[47] There are *numerous* notational conventions for three-level systems. It is also common to define $\Delta_a = \omega_a - (\omega_e^{(0)} - \omega_a^{(0)})$ and $\Delta_b = \omega_b - (\omega_e^{(0)} - \omega_b^{(0)})$, in which case $\delta = \Delta_a - \Delta_b$. As we will see later, one also often sets driving field a to be the (weak) **probe** and b the (strong) **coupling** fields, leading to the notation convention Δ_p and Δ_c ...

7.2 Far-detuned Raman processes

7.2.1 Equivalent two-level system for large detuning

An important class of physics in the three-level system arises when the detuning with respect to the excited state, Δ, is very large compared to the two-photon detuning δ and the Rabi frequencies Ω_a and Ω_b. In this case one can take the formal solution[48] for $c_e(t)$,

$$c_e(t) = -i\int_0^t dt' e^{i\Delta(t-t')}\left[\Omega_a c_a(t') + \Omega_b c_b(t')\right], \tag{110}$$

and assume that the term in brackets varies slowly compared to the exponential and can be taken out of the integral[49] to give

$$c_e(t) \approx \left(\frac{1-e^{i\Delta t}}{\Delta}\right)\left[\Omega_a c_a(0) + \Omega_b c_b(0)\right]. \tag{111}$$

Substituting this into the time-dependent Schrödinger equation [Eq. (109)] reduces it to an effective two-level form

[48] Assuming $c_e(0) = 0$ for convenience, without loss of generality.

[49] If we did this more carefully, it would be termed **adiabatic elimination** of the excited state.

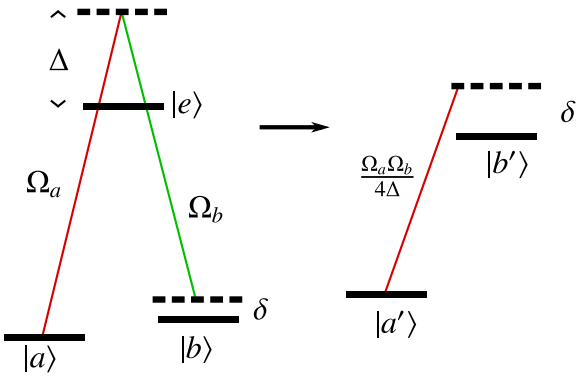

Figure 6: Effective two-level description of a far-detuned Raman process.

$$i\frac{d}{dt}\begin{pmatrix} c_a \\ c_b \end{pmatrix} = \frac{1}{4\Delta}\begin{pmatrix} \Omega_a^2 & \Omega_a\Omega_b \\ \Omega_a\Omega_b & \Omega_b^2 - 4\Delta\delta \end{pmatrix}\begin{pmatrix} c_a \\ c_b \end{pmatrix}, \tag{112}$$

with energy levels $\Omega_{\{a,b\}}^2/4\Delta$ and Rabi frequency $\Omega_a\Omega_b/4\Delta$ [See Fig. 6].

7.2.2 Dark states

For zero two-photon detuning δ, the matrix in the effective two-level Schrödinger equation, Eq. (112), can be written as

$$\frac{1}{4\Delta} = \begin{pmatrix} \Omega_a \\ \Omega_b \end{pmatrix}(\Omega_a\ \Omega_b)\ . \tag{113}$$

In this form, it is straightforward to show that the eigenvectors, and their respective eigenvalues λ, are

$$\mathbf{u}_0 = \begin{pmatrix} -\Omega_b \\ \Omega_a \end{pmatrix},\ \lambda_0 = 0\,; \quad \mathbf{u}_1 = \begin{pmatrix} \Omega_a \\ \Omega_b \end{pmatrix},\ \lambda_1 = \frac{\Omega_a^2 + \Omega_b^2}{4\Delta}\,. \tag{114}$$

Of these, the first eigenvector $\mathbf{u}_0$ is especially notable because it's zero eigenvalue makes it a **dark state**: it no longer directly couples to the light field.

This dark state is in fact preserved if we diagonalize the full three-level Hamiltonian from Eq. (109), to obtain eigenvectors

$$\mathbf{u}_0 = \frac{1}{\Omega_{\text{eff}}}\begin{pmatrix} -\Omega_b \\ 0 \\ \Omega_a \end{pmatrix}; \quad \mathbf{u}_\pm = \frac{1}{\sqrt{4\Omega_\pm^2 + \Omega_{\text{eff}}^2}}\begin{pmatrix} \Omega_a \\ 2\Omega_\pm \\ \Omega_b \end{pmatrix}, \tag{115}$$

where $\Omega_{\text{eff}} = \sqrt{\Omega_a^2 + \Omega_b^2}$ and $\Omega_\pm = [-\Delta \pm (\Omega_{\text{eff}}^2 + \Delta^2)^{1/2}]/2$.

7.2.3 STIRAP

The fact that the nature of the dark state can be manipulated using the two Rabi frequencies Ω_a and Ω_b forms the basis for coherent state manipulation techniques such as Stimulated Raman Adiabatic Passage (STIRAP). The dark state can be expressed as

$$|u_0\rangle = \frac{\Omega_b|a\rangle - \Omega_a|b\rangle}{\Omega_{\text{eff}}}. \tag{116}$$

This expression has the interesting limits of $|u_0\rangle \to |a\rangle$ as $\Omega_a \to 0$ (for $\Omega_b \neq 0$), and $|u_0\rangle \to -|b\rangle$ as $\Omega_b \to 0$ (for $\Omega_a \neq 0$).

These limits allow one to adiabatically move the dark state between $|a\rangle$ and $|b\rangle$ by sufficiently slow tuning of the coupling. A typical STIRAP pulse sequence is shown in Fig. 7. Atoms initially in state $|a\rangle$ adiabatically follow the dark state as the coupling Ω_b is increased. The coupling Ω_a is subsequently increased, and Ω_a reduced to zero, and the dark state becomes $|b\rangle$. Finally, all coupling is reduced to zero, leaving the atoms in state $|b\rangle$.

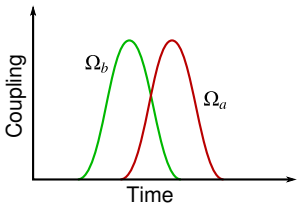

Figure 7: A typical STIRAP pulse sequence.

7.3 EIT and Autler-Townes splitting

Another interesting effect in the three-level system that is connected to the presence of dark states is electromagnetically-induced transparency (EIT). With reference to the Λ system defined by the effective Hamiltonian of Eq. (109), this effect arises when Ω_b represents a strong coupling field and Ω_a a weak probe field. You will investigate this effect, including the effects of spontaneous emission as described by the three-level optical Bloch equations, in Exercise 6.

Exercises 6

EIT and the three-level optical Bloch equations

1. Show that the dark and bright states for the Λ system given in the notes [Eq. (115)] diagonalize the effective Hamiltonian of Eq. (109).

   (*2 marks*)

2. In the Λ EIT configuration, we will use the notation "p" for the weak probe transition from $|a\rangle$ to $|e\rangle$, and "c" for the strongly coupled transition from $|b\rangle$ to $|e\rangle$. This gives effective Hamiltonian

$$H = \frac{\hbar}{2}\begin{pmatrix} 0 & \Omega_p & 0 \\ \Omega_p & -2\Delta_p & \Omega_c \\ 0 & \Omega_c & -2(\Delta_p - \Delta_c) \end{pmatrix}.$$

   Show that the optical Bloch equations for the coherences ρ_{ea}, ρ_{ba}, and ρ_{be} obey the equations

$$\begin{aligned}
\frac{d\rho_{ea}}{dt} &= \frac{i}{2}\Omega_p(\rho_{ee} - \rho_{aa}) + (i\Delta_p - \gamma_{ea})\rho_{ea} - \frac{i}{2}\Omega_c\rho_{ba}\,, \\
\frac{d\rho_{ba}}{dt} &= \frac{i}{2}\Omega_p\rho_{be} + [i(\Delta_p - \Delta_c) - \gamma_{ba}]\rho_{ba} - \frac{i}{2}\Omega_c\rho_{ea}\,, \\
\frac{d\rho_{be}}{dt} &= \frac{i}{2}\Omega_p\rho_{ba} - (i\Delta_c + \gamma_{be})\rho_{be} - \frac{i}{2}\Omega_c(\rho_{ee} - \rho_{bb})\,,
\end{aligned}$$

   where $\gamma_{ij} = (\Gamma_i + \Gamma_j)/2$. Explain the reasoning by which you arrive at the correct form for the dissipative terms.

   (*6 marks*)

3. Show that, for small Ω_p, the steady-state solution for ρ_{ba} is approximately given by

$$\rho_{ba} \approx \frac{1}{2}\left[\frac{i\Omega_c}{i(\Delta_p - \Delta_c) - \gamma_{ba}}\right]\rho_{ea}\,. \tag{117}$$

   (*2 marks*)

4. Using the above result, and assuming that the majority of the population remains in level $|a\rangle$, derive an expression for the steady-state probe coherence ρ_{ea}. Your expression should not include any other density matrix elements.

(*2 marks*)

5. As shown in Section 6 for the two-level atom, the susceptibility of an atomic medium with respect to a coherent light source, χ, is directly proportional to the relevant coherence as determined by the optical Bloch equations (in the two-level case, $\chi \propto \rho_{ge}$). Using the same approach, derive expressions for the real and imaginary parts of the susceptibility of the three-level medium with respect to the EIT probe beam.

(*2 marks*)

6. Using your final expression, plot graphs of the real and imaginary parts of the probe susceptibility as a function of Δ_p/Γ_e for the following coupling Rabi frequencies: $\Omega_c/\Gamma_b = 0, 1/2, 2, 5$. You should set $\Gamma_e/\Gamma_b = 10^4$ (i.e., the decay rate of the excited state is much faster than those for the lower levels), and $\Delta_c = 0$ (i.e., coupling beam on-resonance). Scale your real and imaginary susceptibilities relative to their values when $\Delta_p = \Omega_c = 0$.

(*6 marks*)